Experimental Eye Research 217 (2022) 108953

Contents lists available at ScienceDirect

Experimental Eye Research

journal homepage: www.elsevier.com/locate/yexer

Research article

Minocycline suppresses disease-associated microglia (DAM) in a model of photoreceptor cell degeneration

Ema Ozaki [a,b], Conor Delaney [c], Matthew Campbell [c], Sarah L. Doyle [a,b,d,*]

[a] Department of Clinical Medicine, School of Medicine, Trinity College Dublin, Dublin, Ireland
[b] Trinity College Institute of Neuroscience, Trinity College Dublin, Dublin, Ireland
[c] Smurfit Institute of Genetics, Trinity College Dublin, Dublin, Ireland
[d] National Children's Research Centre, Our Lady's Children's Hospital Crumlin, Dublin, Ireland

ARTICLE INFO

Keywords:
Disease-associated microglia
Minocycline
Retinal degeneration
Lipoprotein lipase

ABSTRACT

As the resident immune cells in the retina, microglia play important homeostatic roles in retinal immune regulation and neuroprotection. However, chronic microglia activation is a common hallmark of many degenerative retinal diseases. The semi-synthetic tetracycline antibiotic, minocycline, appears to inhibit pro-inflammatory microglia which coincides with protection against photoreceptor cell degeneration. A sub-type of microglia termed disease associated microglia (DAM) have recently been associated with a wide range of central nervous system (CNS) diseases. In this study we examine the kinetics of microglia infiltration towards the outer retina of rhodopsin knockout mice (*Rho*$^{-/-}$) by immunofluorescence, and undertake transcriptional and spatial localization analysis of markers for evidence of both homeostatic function and appearance of DAM. We demonstrate in the *Rho*$^{-/-}$ mice, IBA1^{+} and P2RY12^{+} microglia take on an activated morphology early in disease, prior to notable photoreceptor loss and are capable of infiltrating the subretinal space. Expression of lipid processing enzyme and DAM-marker lipoprotein lipase (LPL) is primarily observed only after microglia have traversed the ONL. Administration of minocycline to *Rho*$^{-/-}$ mice induced loss of phagocytic/DAM microglia in the outer retina *in vivo* coinciding with photoreceptor survival and amelioration of retinal degeneration. Overall, we show that minocycline suppresses many DAM markers, in particular those associated with lipid metabolism indicating that suppression of this process is one mechanism by which minocycline protects against inflammation induced photoreceptor cell death.

1. Introduction

Retinal degeneration is a progressive neurodegenerative condition and encompasses a cohort of inherited, acquired and age-related diseases that can lead to severe visual impairment and eventual blindness. Retinitis pigmentosa (RP) is a genetically heterogeneous category of inherited photoreceptor degenerations for which retinal gene therapies targeting X-linked RP with variants in the *RPGR* gene and *RPE65*-related Leber congenital amaurosis (LCA) are proving promising. However, while gene therapies may have benefit for those individuals with mutations in the targeted genes, no broad-spectrum effective treatments exist for this condition. Photoreceptor cells are specialised neurons that convert light into electrical signals that are deciphered in the brain. Identification of unifying processes that can protect photoreceptors from premature death has potential to offer a global therapeutic approach for prolonging sight across multiple inherited blinding diseases.

Retinal inflammation is thought to accelerate the pace of progression of photoreceptor cell death irrespective of the underlying cause of disease, and suppression of microglial activation has been shown to be neuroprotective in mouse models of retinal degeneration (Peng et al., 2014; Zhao et al., 2015; Zabel et al., 2016; Lew et al., 2020; Murakami et al., 2020). Recent advances in single-cell analysis have uncovered subtleties in microglia subtypes that are associated with a wide range of neurodegenerative diseases termed DAM (disease associated microglia) (Keren-Shaul et al., 2017). These DAM appear to be highly effective at phagocytosing debris and unwanted protein aggregates and may in fact be beneficial if triggered early in disease where strong phagocytic activity is desirable.

Recent literature indicates that the semi-synthetic broad spectrum tetracycline antibiotic, minocycline, may have potential to counter-regulate pro-inflammatory microglia and protect photoreceptor cell

* Corresponding author. Department of Clinical Medicine, School of Medicine, Trinity College Dublin, Dublin, Ireland.
E-mail addresses: sarah.doyle@tcd.ie, doyles8@tcd.ie (S.L. Doyle).

https://doi.org/10.1016/j.exer.2022.108953
Received 14 October 2021; Received in revised form 10 January 2022; Accepted 14 January 2022
Available online 25 January 2022

Abbreviations

Apolipoprotein E (APOE)
central nervous system (CNS)
colony stimulating factor 1 (CSF1R)
disease associated microglia (DAM)
external limiting membrane (ELM)
Haemotoxylin and Eosin (H&E)
inner plexiform layer (IPL)
Ionized calcium binding adaptor molecule 1 (Iba1)
Leber congenital amaurosis (LCA)
lipoprotein lipase (LPL)
outer nuclear layer (ONL)
outer plexiform layers (OPL)
Phosphate buffer saline (PBS)
Retinitis pigmentosa (RP)
rhodopsin knockout (*Rho*$^{-/-}$)
Ribonucleic acid (RNA)
sub-retinal space (SRS)
Transmembrane Immune Signalling Adaptor (TYROBP)
Triggering Receptor Expressed On Myeloid Cells 2 (TREM2)
Purinergic Receptor P2Y12 (P2ry12)

degeneration (Peng et al., 2014; Scholz et al., 2015; Di Pierdomenico, Scholz et al., 2018; Gao et al., 2021; Terauchi et al., 2021). As many of these studies in RP animal models such as the *P23H* rat model, *Rd10* mouse model and bright light exposure model are acute models of RP, we were interested to study the rhodopsin knockout (*Rho*$^{-/-}$) mouse model, which manifests as a slower degeneration process over 3 months. The *Rho*$^{-/-}$ retina develops normal numbers of rod and cone nuclei, but the rods have no outer segments and ensuing rod degeneration becomes evident histopathologically from 3 weeks (Ozaki et al., 2020). Rod photoreceptor degeneration is followed by cone photoreceptor degeneration with a complete loss of electrical responsiveness by 8 weeks. At 12 weeks, the majority of photoreceptors in the retina are lost (Humphries et al., 1997). Here, we examine the kinetics of microglia infiltration towards the outer retina of *Rho*$^{-/-}$mice at multiple timepoints throughout the degeneration process, and undertake transcriptional and spatial localization analysis of markers for evidence of both homeostatic function and appearance of DAM. Administration of minocycline to *Rho*$^{-/-}$ mice reduced markers of DAM in the degenerating retina and prevented microglial infiltration into the SRS. This loss of DAM microglia in the outer retina *in vivo* coincides with photoreceptor survival and amelioration of retinal degeneration.

2. Materials and methods

2.1. Animals

All animal studies were carried out in accordance to the principles laid out by the internal ethics committee at TCD, and all relevant national licenses were obtained before commencement of work. C57BL/6J mice were obtained from Jackson Laboratory and bred on-site and *Rho*$^{-/-}$ mice were kindly provided by Prof Peter Humphries, TCD. Animals were kept on a 12-h light/dark cycle and both male and female mice were used in this study.

2.2. Minocycline administration

Rho$^{-/-}$ mice received intra-peritoneal injections of 50 mg/kg minocycline (Sigma-Aldrich) or vehicle H_2O twice daily, starting from postnatal day 16 and continuing till postnatal day 21 or 42.

2.3. H&E staining

Eyes were fixed in Davidson's Fixative for 24 h, dehydrated and immersed in molten wax in a tissue processor (1 h 70% ethanol, 1 h 80% ethanol, 1 h 95% ethanol, 1 h 100% ethanol, 1 h 100% ethanol, 1 h 50% ethanol/xylene, 1 h xylene, 1 h xylene, 1 h paraffin at 60 °C and 1 h paraffin under vacuum at 60 °C) before being embedded in paraffin. Using a microtome, 5 μm sections were collected onto Polysine slides. Paraffin sections were deparaffinised and rehydrated by dipping 10 times each in xylene, 100%, 90% and 70% ethanol. Slides were immersed in haemotoxylin for 6 min, rinsed in water, and then immersed in eosin for 2 min and rinsed in water. Slides were dehydrated by dipping 10 times in 70%, 90%, 100% ethanol and xylene before being mounted with coverslips using Sub-X Mounting Medium. H&E images were acquired on a light microscope (Olympus 1X81).

2.4. Immunohistochemistry of retinal cryosections

Eyes were fixed in 4% paraformaldehyde (PFA) at room temperature for 1.5 h, followed by the removal of the cornea and lens. Eyes were cryoprotected under a 20% and 30% sucrose gradient overnight at 4 °C, and subsequently frozen in optimum cutting temperature compound. Using a cryostat, 12 μm sections were collected onto Polysine. Retinal cryosections were blocked/permeabilized with 5% normal goat serum (NGS) and 0.05% Triton X-100 in PBS for 1 h at room temperature. Sections were incubated with primary antibody diluted in 5% NGS at 4 °C overnight. Primary antibodies used were IBA1 (Wako, 019–19741, 1:500), CD68 (Abcam, ab53444, 1:200), P2RY12 (AnaSpec ANA55043A, 1:100), and LPL (Abcam, ab21356, 1:100). Following 3 washes in PBS, slides were incubated with Alexa Fluor 594- and 488-conjugated goat anti-rabbit, Alexa Fluor 488-conjugated anti-mouse and Alexa Fluor 594-conjugated anti-rat secondary antibodies (1:500; Invitrogen) diluted in 5% NGS for 2 h at room temperature. Sections were counterstained with Hoechst 33342 (1:10,000) before being mounted with coverslips using Hydromount (VWR) mounting medium. Images were acquired using a confocal microscope (Zeiss LSM 710) and area of IBA1^{+} staining was analysed using *ImageJ* and averaged over 6 sections per mouse.

2.5. Immunohistochemistry of retinal flatmounts

Following fixation in 4% PFA for 15 min, the cornea and lens were removed, and 4 incisions were made into the retinal eye cup to flatten out the tissue. The tissue was fixed for a further 15 min in 4% PFA and then washed 3 times in PBS. Retinal flatmounts were blocked/permeabilized with 10% NGS and 1% Triton X-100 in PBS at 4 °C overnight and subsequently incubated with IBA1 antibody for 48 h at 4 °C. After 3 washes in PBS, flatmounts were incubated with Alexa Fluor 594-conjugated anti-rabbit secondary antibody at 4 °C overnight before being mounted with coverslips using Hydromount (VWR) mounting medium. Images were acquired using a confocal microscope (Zeiss LSM 710) and analysed using *ImageJ*.

2.6. Cell culture

The mouse microglial BV2 cell line was cultured in RPMI with 10% FBS, supplemented with 10% fetal bovine serum (Sigma-Aldrich) and 1% penicillin/streptomycin (Sigma-Aldrich) and maintained at 37 °C in a humidified 5% CO_2 atmosphere. The cells were seeded at 5×10^4 cells per cm^2 and incubated overnight before treatment. BV2 cells were treated with 5 μg/ml minocycline or sterile H_2O as vehicle control. Cells were harvested 6 h and 24 h after treatment.

2.7. Phagocytosis assay

BV2 cells were plated on chamber slides and treated with 5 μg/ml

minocycline for 21 h prior to being assayed. Polystyrene amine modified (yellow-green) latex beads (Sigma-Aldrich) were pre-opsonized in FBS (1:5) at 37 °C for 1 h. Opsonized beads were diluted 1:2000 in media and added to cells for 3 h. Cells were washed with ice-cold PBS 3 times to remove surface bound beads, fixed in 4% PFA for 10 min and stained with MitoTracker Orange CMTMRos for 30 min. Cells were washed and counterstained with Hoechst 33342 (1:10,000). Cells were imaged on a BX51 Olympus microscope and analysed by ImageJ.

2.8. qRT-PCR analysis

RNA was extracted from BV2 cells or mouse retinas using Isolate II RNA extraction kit (Bioline) as per the manufacturer's instructions and made into cDNA using MMLV Reverse Transcriptase (Promega). RT-PCR was performed using SensiFast SYBR Green (Bioline) on the ABI 7900HT system (Applied Biosystems). The comparative delta-delta CT method was used for to quantify relative mRNA changes with normalisation to the housekeeping gene ubiquitin C (UBC). Primer sequences used were as follows:

Target	Forward Primer (5′-3′)	Reverse Primer (5′-3′)
Apoe	ATTGCTGACAGGATGCCTAGC	GGTTGGTTGCTTTGCCACTC
Axl	TTCAACTGTGCTACGTCCCC	GGGTCCCTCTAGGTAAGCCA
Clec7a	GTGGTAGTAGTGGTTGCTGC	ATTCTGTGGGCTTGTGGTTC
Csf1r	AAGCAGAAGCCGAAGTACCA	GTCCCTGCGCACATATTTCAT
Ctsb	CAGGCTGGACGCAACTTCTA	GCCCCAAATGCCCAACAAG
Cx3cr1	CTGTTATTTGGGCGACATTG	AACAGATTTCCCACCAGACC
Inos	ATGGACCAGTATAAGGCAAGC	GCTCTGGATGAGCCTATATTG
Itgax	CGATGCCTTCCCATGAATACG	CTTGGTGTCTCTGTGCCCTC
Lgals3	CTCTGACAGCTAGCGGAGC	AGGCATCGTTAAGCGAAAAGC
Lpl	TCGTCATCGAGAGGATCCGA	TGTTTGTCCAGTGTCAGCCA
P2ry12	CAAGGGGTGGCATCTACCTG	AGGCAGCCTTGAGTGTTTCTG
Sall1	TTTCCAATCCGACCCCGAAG	CCACAGACATGGGCATCCTT
Selplg	GGGATGGTCCTTCCTTTGGG	ACAATGGTCTAAGCGCCCTC
Spp1	CTGGCTGAATTCTGAGGGACT	CTGCTTCTGAGATGGGTCAGG
Tgfbr1	AGCTCCTCATCGTGTTGGTG	GGCCTGTCTCGAGGAATTAGG
Tmem119	TTCACCCAGAGCTGGTTCCATA	TCTCCGGTGTGGGACTGAA
Trem2	ACAGCACCTCCAGGAATCAAG	AGGATCTGAAGTTGGTGCCC
Tyrobp	GGTGTACTGGCTGGGATTGT	GCAATGTGTTGTTTCCGGGT
Ubc	CCCAGTGTTACCACCAAGAAG	CCCCATCACACCCAAGAACA

2.9. Western blot analysis

Retinal tissue and BV2 cells were lysed in RIPA lysis buffer with phosphatase and protease inhibitors (Sigma-Aldrich) and centrifuged at 15,000 *g* for 15 min. 10 μg of protein was resolved on 10% or 12% SDS polyacrylamide gels before being transferred onto a PVDF membrane and blocked in 5% non-fat milk in Tris-buffered saline containing 0.05% Tween-20 (TBST) for 1 h. Membranes were incubated in primary antibodies against APOE (Merck, 178479, 1:2000), LPL (Abcam, ab21356, 1:1000), Galectin-3 (R&D, AF1197, 1:2000), CSF1R (Invitrogen, PA5-25974, 1:500) and β-actin (1:2000; Sigma-Aldrich) overnight at 4 °C, washed 3 times in TBST, and incubated in horseradish peroxidase–conjugated anti-rabbit, anti-mouse or anti-goat secondary antibodies (1:2000; Sigma-Aldrich) for 1 h at room temperature. Following 3 washes in TBST, the membranes were visualised using enhanced chemiluminescence (Advansta) in a dark box. Densitometry was performed on *ImageJ*, with proteins normalized to the loading control β-actin.

3. Results

3.1. Microglia are activated and infiltrate the outer retina in the $Rho^{-/-}$ model of photoreceptor degeneration

Microglia are morphologically and functionally dynamic cells that can transform from a highly ramified state into a rod or amoeboid state during activation and pathology. Under basal or physiological conditions, ramified microglia predominate. However, in response to injury or inflammatory conditions, de-ramification occurs where microglial processes shorten and thicken and cell bodies expand, ultimately shifting into a round amoeboid shape (Karperien et al., 2013). Here, we examine microglia dynamics in the $Rho^{-/-}$ model of retinal degeneration. $Rho^{-/-}$ mice develop a normal number of rod and cone nuclei but with the absence of rod outer segments (OS), these cells begin to degenerate from 3 weeks of age and by 12 weeks most of the photoreceptors are lost. To visualize and characterize the role of microglia in the $Rho^{-/-}$ model of retinal degeneration we performed immunofluorescence on retinal flat-mounts of the microglia marker IBA1 in wild-type and $Rho^{-/-}$ mice at 3, 6, 9 and 12 weeks of age (Fig. 1A). At all time-points observed, wild-type microglia had a ramified appearance with long fine processes and small cell bodies indicative of physiological 'surveillant' microglia (Fig. 1A, first column). In the contrary, microglia in the $Rho^{-/-}$ retinal flat-mounts had an activated appearance with larger cell bodies and retracted processes (Fig. 1A, second column), which are particularly evident in the high magnification and skeleton images (Fig. 1A, a'-h'). De-ramified microglia were evident from as early as 3 weeks of age (Fig. 1A, a', b'), demonstrating that microglial activation occurs from a very early age in the $Rho^{-/-}$ mice. To examine the distribution of microglia within the laminar structure of the retina in the $Rho^{-/-}$ mice, we stained cross sections of the retina from these mice at 3, 6, 9 and 12 weeks of age with IBA1. In the wild-type retina, IBA1-stained microglia were observed in the synaptic inner plexiform (IPL) and outer plexiform layers (OPL) (Fig. 1B, first column). However, in the retinal cryosections from $Rho^{-/-}$ mice, IBA1-stained microglia were seen to migrate into the outer nuclear layer (ONL) and down towards the photoreceptor inner and outer segments or sub-retinal space (SRS) (Fig. 1B, second column).

3.2. Microglia infiltrating the SRS are actively phagocytosing photoreceptor cells and express disease associated microglia (DAM) marker LPL

Next, we sought to analyse the microglia infiltrating the SRS for markers of phagocytosis and markers of homeostatic function. First, we stained retinal cryosections from 12 week old wild-type mice (Fig. 2A, top row) and $Rho^{-/-}$ mice at 3, 6, 9 and 12 weeks of age with CD68, a lysosomal protein that is upregulated in actively phagocytic cells. In wild-type sections, no co-localization of CD68 and IBA1 were observed, and fluorescence was mainly seen in the OPL likely due to non-specific IgG staining in the blood vessels (Fig. 2A, top row). CD68 positive staining was significantly increased in $Rho^{-/-}$ cryosections and co-localization of IBA1 and CD68 was observed in microglia in the OPL and in microglia that had infiltrated the ONL and SRS (Fig. 2A a' & 2A b'). As IBA1 is also expressed in macrophages, we next stained retinal cryosections with the more recently identified microglial-specific homeostatic marker P2RY12 (Fig. 2B). Although some studies have found a decrease in microglial homeostatic genes like P2RY12 in aging and neurodegenerative models, we found P2RY12 immunopositivity in both wild-type cryosections (Fig. 2B, top row) and $Rho^{-/-}$ cryosections at 3, 6, 9 and 12 weeks of age (Fig. 2B, **rows 2–5**). Co-staining with CD68 also revealed co-localization of CD68 and P2RY12 in the activated microglia in the OPL, ONL and SRS of $Rho^{-/-}$ mice (Fig. 2B a' and 2B b'). Finally, retinal cryosections from wild-type and $Rho^{-/-}$ mice were stained with lipoprotein lipase (LPL) (Fig. 3). LPL, an enzyme that hydrolyses triglyceride rich lipoproteins, is associated with an alternatively activated and highly phagocytic microglial phenotype. In wild-type retinas, no LPL reactivity was observed in microglia with fluorescence only observed in blood vessels (either due to non-specific IgG staining or specific staining of vessel walls) (Fig. 3A). In contrast, LPL immunopositivity was observed in $Rho^{-/-}$ retinas at 3, 6, 9 and 12 weeks of age and co-staining with IBA1 revealed co-localization with microglia that resided solely in the SRS; $IBA1^{+}$ microglia in the inner retina remained LPL-negative (Fig. 3A a' b' c' & d', white arrows).

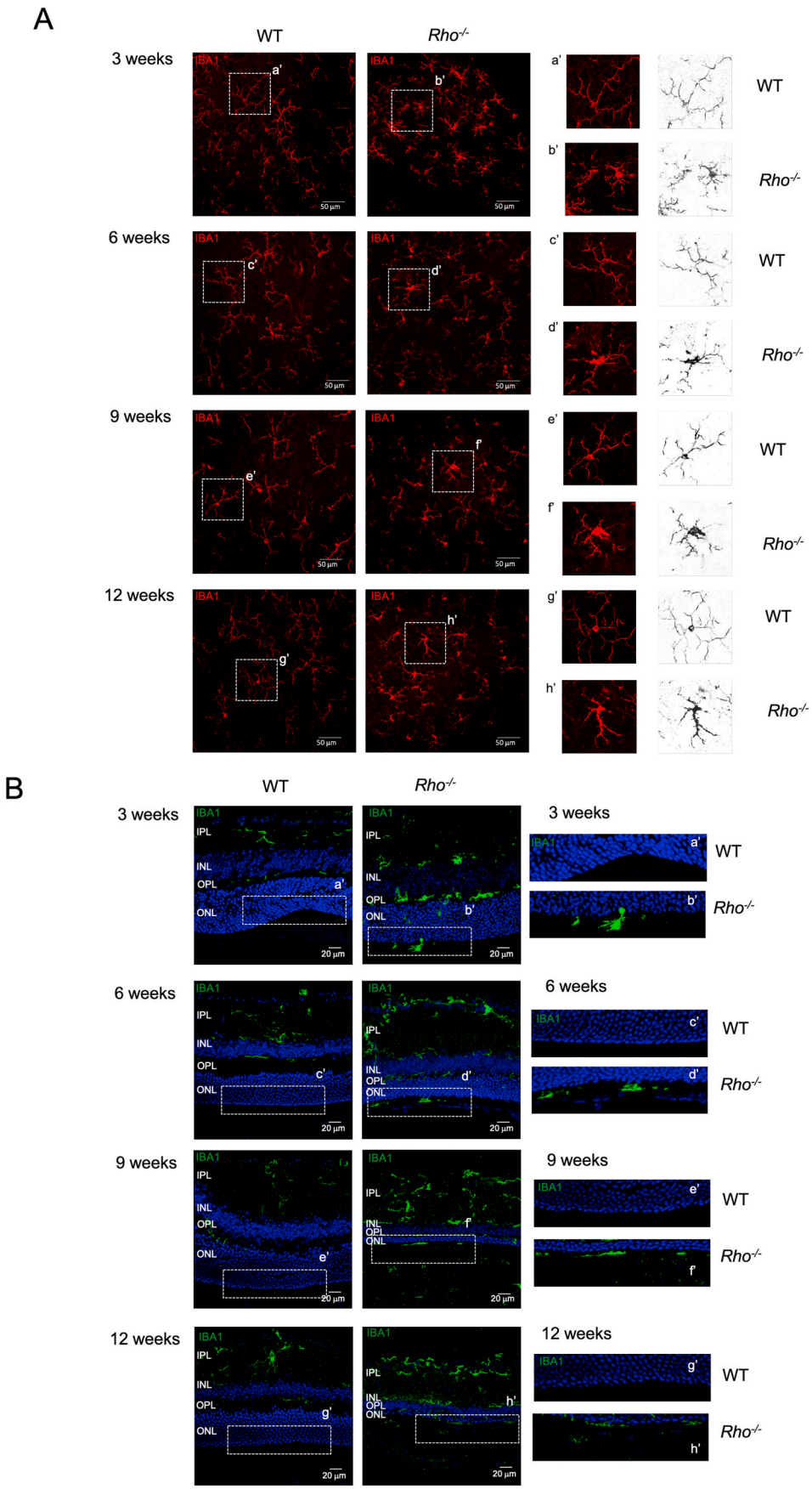

Fig. 1. Microglia are activated and infiltrate the outer retina over time in the *Rho*$^{-/-}$ model of photoreceptor degeneration.
(**A**) Retinal flat-mounts from WT and *Rho*$^{-/-}$ mice at 3, 6, 9 and 12 weeks of age stained with the microglia marker IBA1 (20X magnification) with (**a'-h'**) magnified and skeleton images. (**B**) Retinal cryosections from WT and *Rho*$^{-/-}$ mice at 3, 6, 9 and 12 weeks of age stained with the microglia marker IBA1 (40X magnification, nuclei staining - Hoechst), with (**a'-h'**) magnified images of the ONL and sub-retinal space shown to the right. (IPL – inner plexiform layer, INL – inner nuclear layer, ONL outer nuclear layer).

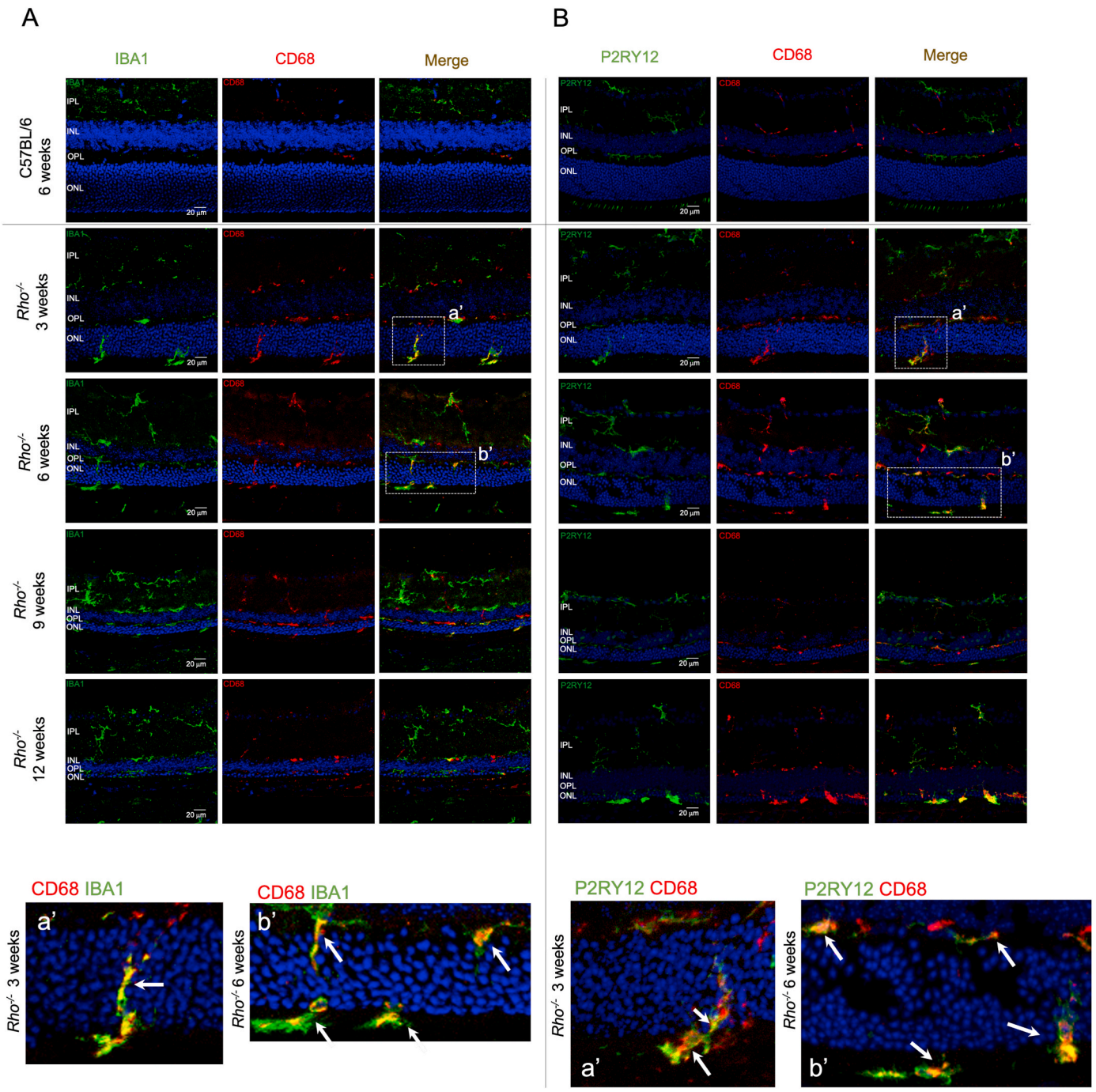

Fig. 2. Microglia infiltrating the sub-retinal space are actively phagocytosing photoreceptor cells.
(**A**) Retinal cryosections from WT mice and *Rho*$^{-/-}$ mice at 3, 6, 9 and 12 weeks of age stained with IBA1 and CD68 (40X magnification) with magnified images of *Rho*$^{-/-}$ mice at (**a'**) 3 and (**b'**) 6 weeks. (**B**) Retinal cryosections from WT mice and *Rho*$^{-/-}$ mice at 3, 6, 9 and 12 weeks of age stained with P2RY12 and CD68 (40X magnification) with magnified images of *Rho*$^{-/-}$ mice at (**a'**) 3 and (**b'**) 6 weeks (nuclei staining - Hoechst, arrows indicate areas of co-staining). (IPL – inner plexiform layer, INL – inner nuclear layer, ONL outer nuclear layer, LPL – lipoprotein lipase).

3.3. Minocycline downregulates DAM genes in the Rho$^{-/-}$ *model of retinal degeneration*

Minocycline, a broad-spectrum tetracycline antibiotic, has previously been reported to ameliorate photoreceptor cell death in numerous mouse models of retinal degeneration (Zhang et al., 2004; Kohno et al., 2013; Peng et al., 2014; Scholz et al., 2015; Dannhausen et al., 2018; Terauchi et al., 2021) and is a known inhibitor of microglial activation. Given the interesting LPL staining pattern we had observed in the *Rho*$^{-/-}$ retina, we wanted to examine the effects of minocycline on genes associated with homeostatic function and those that are a signature of DAM. DAM-related genes of which LPL is a key member have been revealed due to recent advances in single cell technologies. We injected *Rho*$^{-/-}$ mice with 50 mg/kg of minocycline or vehicle (H_2O) control twice a day from post-natal day 16 (P16) until the mice were sacrificed at 3 weeks of age. Immunofluorescence of IBA1 in retinal flat-mounts from these mice showed a significant reduction in activated microglia with minocycline treatment, with the cells having a more ramified morphology compared to vehicle injected mice (Fig. 4A). The difference in morphology was confirmed using the grid cross method where the

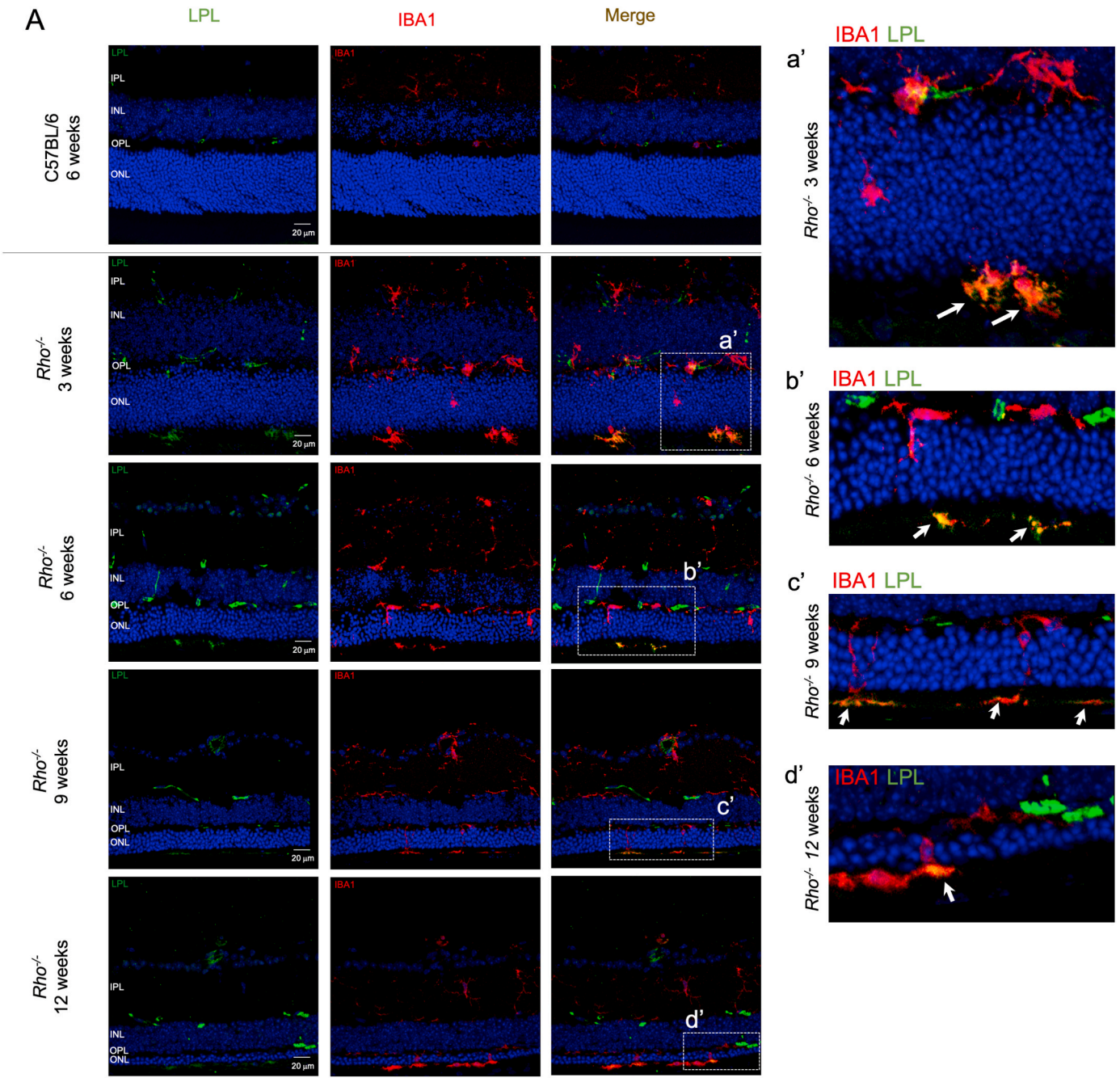

Fig. 3. Microglia infiltrating the sub-retinal space express DAM marker LPL.
(**A**) Retinal cryosections from WT mice and *Rho*$^{-/-}$ mice at 3, 6, 9 and 12 weeks of age stained with IBA1 and LPL (40X magnification) with magnified images of *Rho*$^{-/-}$ mice at (**a'**) 3, (**b'**) 6, (**c'**) 9 and (**d'**) 12 weeks (nuclei staining - Hoechst, arrows indicate areas of co-staining). (IPL – inner plexiform layer, INL – inner nuclear layer, ONL outer nuclear layer, LPL – lipoprotein lipase).

ramified microglia from minocycline-injected animals had greater numbers of grid cross points compared to the shorter cellular processes of the vehicle injected *Rho*$^{-/-}$ mice (Fig. 4B). We then assessed the neural retina of minocycline or vehicle injected *Rho*$^{-/-}$ mice for signature markers of homeostatic microglia and DAM. Out of the 6 homeostatic microglial genes (*Cx3cr1, P2ry12, Sall1, Tgfbr1, Selplg, Tmem119*) assessed by quantitative real-time PCR, expression levels of 5 remained unchanged while *Sall1* was found to be downregulated in retinas from minocycline-injected mice (Fig. 4C). Interestingly, the DAM signature genes (*Apoe, Axl, Clec7a, Ctsb, Csf1r, Itgax, Lgals3, Lpl, Spp1, Trem2, Tyrobp*) were found to be more transcriptionally dynamic with a reduction in *Apoe*, *Axl*, *Clec7a*, *Csf1r*, *Ctsb* and *Lpl* levels in retinas from minocycline injected mice while *Itgax* levels increased (Fig. 4C). The gene expression profiles of these microglial genes are illustrated in a heatmap (Fig. 4D) with genes most highly expressed in the retina in red and those least expressed in blue. As one of the most significantly downregulated DAM genes by minocycline at the transcriptional level, LPL levels were further examined in retinal cryosections from these mice. In vehicle-injected 3-week-old *Rho*$^{-/-}$ mice, LPL and IBA1 co-localization was observed in microglia residing in the SRS whereas LPL was absent in all microglia in minocycline injected animals (Fig. 4E).

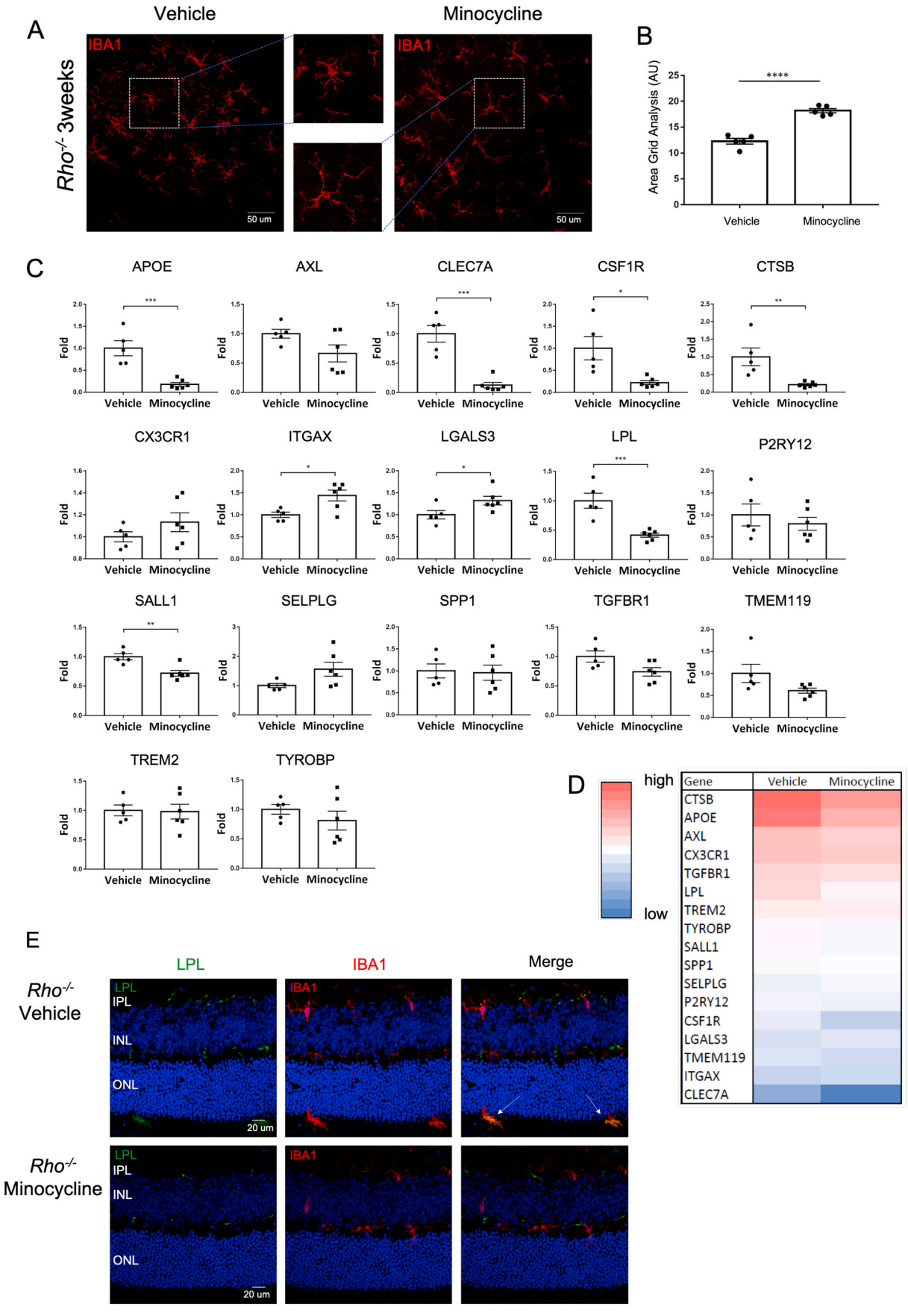

(caption on next page)

Fig. 4. Minocycline regulates microglia activation, downregulating DAM genes in the *Rho*$^{-/-}$ model of retinal degeneration.
(**A**) IBA1-stained retinal flat-mounts from *Rho*$^{-/-}$ mice at 3 weeks of age given intra-peritoneal injections of vehicle or minocycline (50 mg/kg) twice daily from post-natal day 16 (P16) to P21 with (**B**) microglial activation quantified by area grid analysis. (**C**) RT-qPCR analysis of homeostatic and DAM gene transcript levels in the neural retina from these minocycline- or vehicle-injected *Rho*$^{-/-}$ mice at 3 weeks of age with a (**D**) heatmap showing the level of expression normalised to the housekeeping gene ubiquitin C (*$P \leq 0.05$, **$P \leq 0.01$, ***$P \leq 0.001$ by *t*-test, $n = 5$–6 mice). (**E**) Retinal cryosections from these minocycline- or vehicle-injected *Rho*$^{-/-}$ mice at 3 weeks of age stained with IBA and the DAM gene LPL. (IPL – inner plexiform layer, INL – inner nuclear layer, ONL outer nuclear layer, LPL – lipoprotein lipase).

3.4. Minocycline regulates DAM gene expression in BV2 microglia in vitro

As the neural retina is composed of many different cell types, we next sought to examine how minocycline affects homeostatic and DAM gene expression profiles specifically in microglia, using the BV2 mouse microglia cell line. Minocycline is known to inhibit M1 polarization in microglia (Kobayashi et al., 2013) so we first confirmed by quantitative real-time PCR analysis that transcriptional levels of the M1 marker iNOS was significantly reduced in BV2 cells after minocycline (5 μg/ml) treatment (Fig. 5A 1st panel). Interestingly, we saw no significant changes in the 6 homeostatic microglial genes (*Cx3cr1, P2ry12, Sall1, Tgfbr1, Selplg, Tmem119*) assessed while minocycline significantly reduced 3 of the DAM genes, *Clec7a*, *Lpl* and *Tyrobp* (Fig. 5A). Again, the gene expression profiles of these microglial genes are illustrated in a heatmap (Fig. 5B) with the most highly expressed genes in red and the least expressed in blue. Next, we investigated whether minocycline could alter the protein expression levels of some of these microglial markers by Western blot analysis. Similar to what was observed at the transcriptional level, minocycline significantly reduced LPL protein expression (Fig. 5C, top row & Supplementary Fig. 1A). As LPL is a key

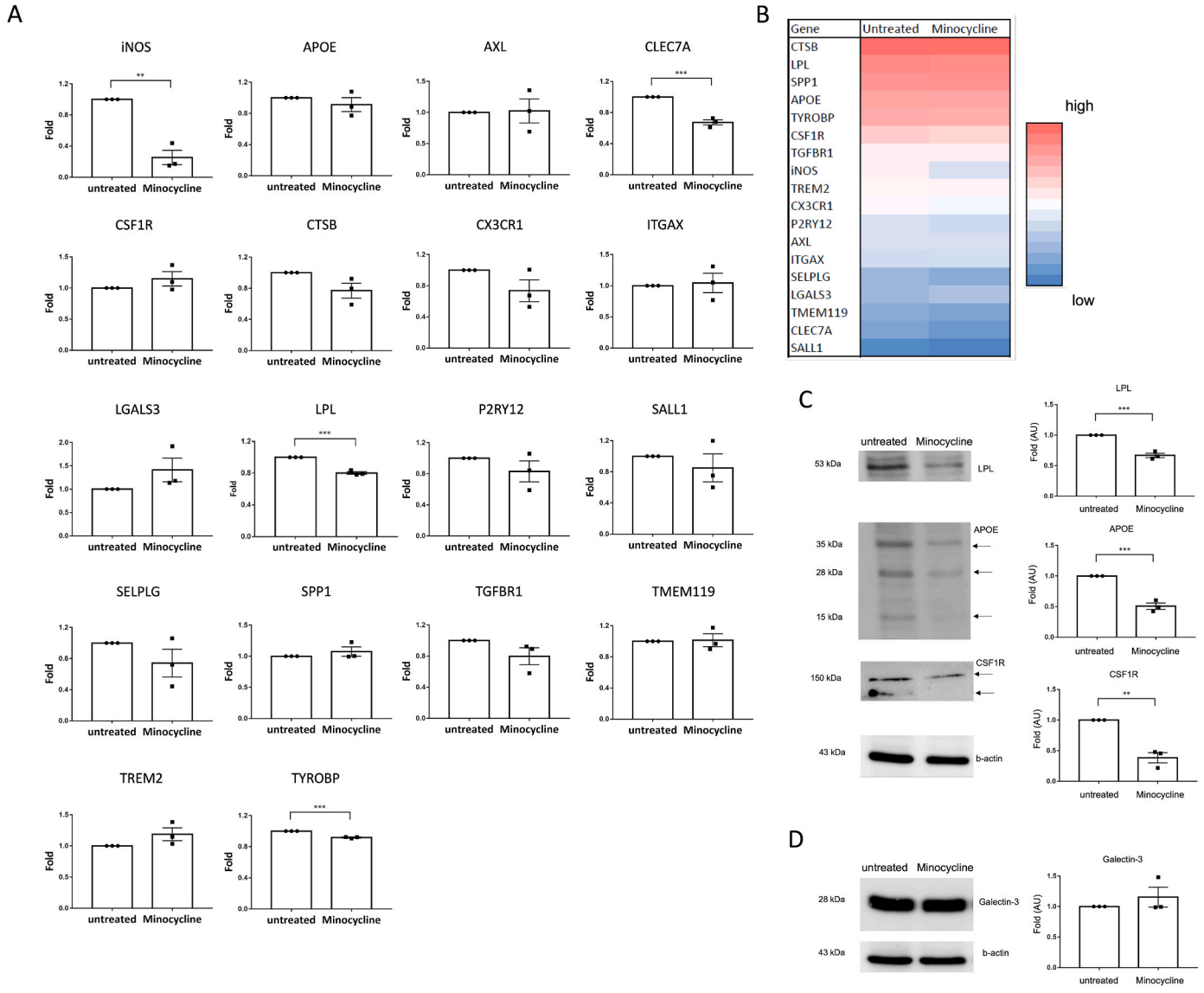

Fig. 5. Minocycline directly regulates DAM gene expression in BV2 microglia *in vitro*.
(**A**) RT-PCR analysis of homeostatic and DAM gene transcript levels in BV2 microglial cells that were untreated or treated with 5 μg/ml minocycline for 7 h with a (**B**) heatmap showing the level of expression normalised to the housekeeping gene ubiquitin C (***$P \leq 0.001$ by *t*-test, $n = 3$ biological replicates). (**C, D**) Western blot analysis of LPL, APOE, CSF1R and Galectin-3 expression levels in BV2 microglial cells that were untreated or treated with 5 μg/ml minocycline for 24 h with densitometry shown to the right (**$P \leq 0.01$, ***$P \leq 0.001$ by *t*-test, $n = 3$ biological replicates).

enzyme involved in lipid metabolism, we also examined levels of apolipoprotein E (APOE), a lipid and cholesterol transporter that is prominently associated with neurodegenerative disease. Although we did not see any changes in *Apoe* at the transcriptional level in BV2 cells, minocycline significantly reduced both 34-kDa full-length APOE protein as well as APOE fragments observed at 28- and 15-kDa (Fig. 5C, middle row & Supplementary Fig. 1B). CSF1R (colony stimulating factor 1) levels were also significantly decreased by minocycline (Fig. 5C, bottom row & Supplementary Fig. 1D), despite not being altered at the transcriptional level. CSF1R is a primary regulator of microglial proliferation, migration, differentiation and survival and has been found to be upregulated in inflammatory and neurodegenerative disease. Finally, we looked at protein levels of the DAM marker Galectin-3. *Lgasl3*, the gene encoding galectin-3, was significantly upregulated in the minocycline injected $Rho^{-/-}$ retinas, however, protein levels remained unchanged in minocycline treated BV2 cells (Fig. 5D & Supplementary

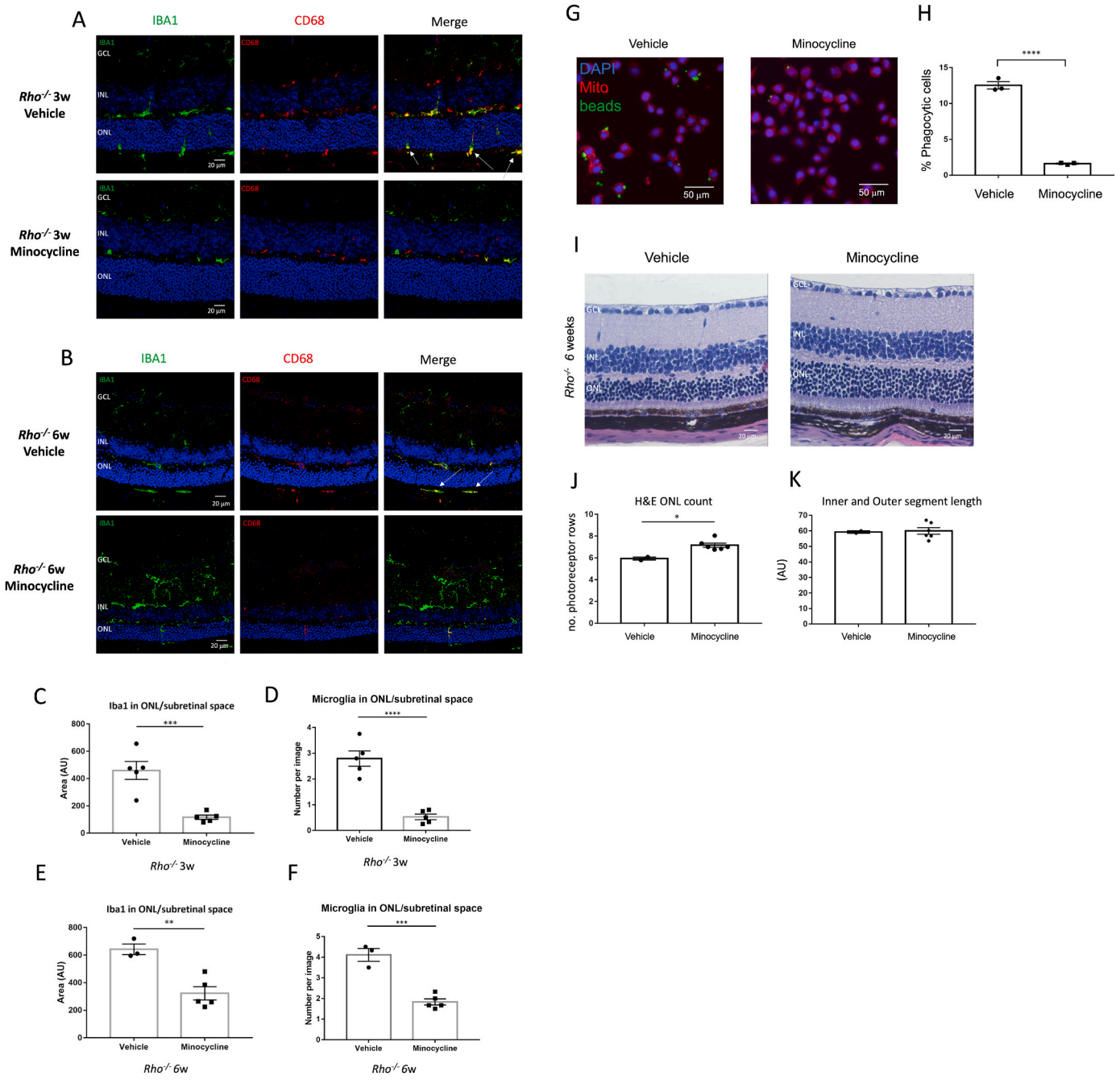

Fig. 6. Minocycline inhibits microglial phagocytic function and supports photoreceptor survival in the $Rho^{-/-}$ model of retinal degeneration.
(**A, B, C, D, E, F**) IBA1-and CD68-stained retinal cryosections from $Rho^{-/-}$ mice at 3 weeks and 6 weeks of age given intra-peritoneal injections of vehicle or minocycline (50 mg/kg) twice daily from post-natal day 16 (P16) to P21 or from P16 to P42 with microglia residing in SRS and the ONL quantified by area and number ($^{**}P \leq 0.01$, $^{***}P \leq 0.001$ $^{****}P \leq 0.0001$ by *t*-test) (**G**) Immunocytochemistry of BV2 microglial cells that were untreated or treated with 5 μg/ml minocycline for 24 h and exposed to fluorescent opsonised latex beads for 3 h before fixation and stained with MitoTracker and Hoechst. (**H**) Quantification of BV2 phagocytic activity expressed as percentage of bead^{+} cells ($^{***}P \leq 0.001$ by *t*-test, data representative of 3 separate experiments with 3 fields of view imaged per well). (**I, J, K**) Haemotoxylin and eosin staining of paraffin-embedded sections from these minocycline- or vehicle-treated $Rho^{-/-}$ mice at 6 weeks with quantification of the number of photoreceptor rows in the ONL and inner and outer segment length ($^{*}P \leq 0.05$, $n = 3$–6 mice per group). (GCL – ganglion cell layer, INL – inner nuclear layer, ONL outer nuclear layer).

Fig. 1E).

3.5. Minocycline inhibits microglial phagocytic function and supports photoreceptor survival in the *Rho*$^{-/-}$ retinal degeneration model

It was clear that minocycline reduced LPL-positive microglia in the SRS of the *Rho*$^{-/-}$ retina (Fig. 4E). We sought to further examine the effect of minocycline on microglia migration. Retinal cryosections from *Rho*$^{-/-}$ mice that had received two daily injections of minocycline or vehicle control from P16 to P21 or P42, were stained with IBA1 and CD68 to more broadly mark actively phagocytosing cells. IBA1^{+} microglial cells were clearly observed in the IPL, OPL, ONL and SRS in vehicle injected mice, but the number of IBA1^{+} cells in the ONL and SRS was significantly reduced in mice treated with minocycline at both 3 weeks (Fig. 6A, 6C & 6D) and 6 weeks (Fig. 6B, 6E & 6F) of age, with the majority of microglia residing in the IPL and OPL. Both the area and number of IBA1^{+} cells occupying the ONL and subretinal space were measured, averaged across 6 images per mouse taken from cryosections cut on a sagittal plane through the optic nerve head. Furthermore, co-localization of CD68 and IBA1 was evident in the OPL, ONL and SRS in vehicle injected mice, but this was greatly reduced in minocycline-injected animals. As the majority of cells that were CD68^{+}IBA1^{+} double-positive were those that had migrated towards the dying photoreceptors, it was difficult to decipher whether minocycline was simply slowing down the migration of these cells towards the SRS or whether minocycline was directly reducing the cells' phagocytic ability. To overcome this we examined whether minocycline could alter the phagocytic capacity of microglia *in vitro*. Untreated and minocycline-treated BV2 cells were incubated with green fluorescent latex beads for 3 h and internalisation of the beads was measured by immunofluorescence (Fig. 6G). Indeed, minocycline treatment resulted in a marked reduction in the number of BV2 cells that had engulfed the latex beads compared to untreated cells (Fig. 6H), indicating that minocycline could directly reduce the basal phagocytic capacity of these cells.

Finally, we assessed the therapeutic efficacy of minocycline administration in our *Rho*$^{-/-}$ model. As before, minocycline was administered by two daily injections from P16 to P42 and we examined photoreceptor cell death by H&E staining of paraffin-embedded retinal tissue sections from these mice. We counted the number of nuclei rows in the ONL of each eye at 12 points along the vertical meridian from sections cut on a sagittal plane through the optic nerve head at ~150 and ~250 μm from the periphery (Fig. 6I). ONL counts indicated minocycline attenuated photoreceptor cell death in the *Rho*$^{-/-}$ mice with a significant preservation of the number of photoreceptor rows still remaining at 6 weeks of age (Fig. 6J). Quantification of the distance from the RPE to the external limiting membrane demonstrated no significant changes with minocycline treatment, indicating that minocycline preserves photoreceptor cell numbers and not the length of the inner segments of the rods, and inner and outer segments of the cones (Fig. 6K).

4. Discussion

As the resident immune cells in the retina, microglia play important homeostatic roles in retinal immune regulation and neuroprotection. Studies have shown that inhibiting microglial function leads to the accumulation of debris and apoptotic cells accelerating photoreceptor degeneration (Okunuki et al., 2018; Silverman et al., 2019). However, conversely, under continuous pathological insult, uncontrolled and chronic microglia activation ensues, and is a common hallmark of many degenerative retinal diseases (Peng et al., 2014; Zhao et al., 2015; Zabel et al., 2016; Lew et al., 2020). Here, we investigate how minocycline, a semi-synthetic tetracycline analogue, affects molecular signatures of homeostatic and DAM *in vivo* using the *Rho*$^{-/-}$ model of retinal degeneration and *in vitro* using the murine microglia BV2 cell line. Due to the recent surge in single cell RNA transcriptomics, microglia signatures in homeostatic versus diseased phenotypes have been well defined, identifying this DAM subtype. The activation of homeostatic microglia into DAM is a two-step process, with a clear intermediary state observed. In the initial stage, there is a downregulation of microglial homeostatic genes (*e.g. P2ry12, Cx3cr1, Tmem119, Tgfbr1*) along with the upregulation of a subset of DAM genes (*e.g. Tryobp, Apoe, B2m and Ctsb*). Induction of the key genes involved in lipid metabolism and phagocytosis (*e.g. Lpl, Itgax, Clec7a, Trem2*) are not observed until the second stage of DAM activation, a stage which is dependent on TREM2 signalling (Keren-Shaul et al., 2017).

Here, we found that microglia are activated and infiltrate the outer retina in the *Rho*$^{-/-}$ model, and this is observed from even 3 weeks of age at the onset of photoreceptor cell death. These microglia infiltrating the SRS are actively phagocytosing and express the DAM marker LPL. Surprisingly, LPL appears only to be present in microglia residing in the lipid rich environment in the inner and outer segments. Even on traversing through the ONL, we observe no LPL positive stain on the inner retinal side of the external limiting membrane (ELM), despite these microglia being positive for the phagocytic marker CD68; CD68 is apparent in IBA1^{+} and P2RY12^{+} cells in the INL prior to deeper infiltration into the outer retina. Of note, LPL has been shown to co-localize with microglia that have internalized amyloid beta (Aβ) in mouse and human brains (Keren-Shaul et al., 2017), suggesting that LPL plays a direct role in Aβ uptake and perhaps, in our *Rho*$^{-/-}$ model, only the microglia that have already phagocytosed the photoreceptor segments in the SRS are LPL positive.

Minocycline has been widely used in CNS studies as a microglial inhibitor, however, its effect on the DAM profile has never been investigated. Thus, we next explored whether minocycline could modify DAM signature genes in the retina of *Rho*$^{-/-}$ mice as well as in BV2 microglial cells directly. Interestingly, we found that *Sall1* levels showed a decrease with minocycline treatment in *Rho*$^{-/-}$ animals while the remainder of the homeostatic genes, *P2ry12, Cx3cr1, Tmem119, Tgfbr1* and *Selplg* remained unchanged. *Sall1* encodes a transcription regulator that dampens a reactive microglia phenotype allowing them to conduct their physiological functions (Buttgereit et al., 2016), so it is surprising that this gene was down-regulated with minocycline. However, minocycline did not directly alter this or any other homeostatic genes in microglia *in vitro*. It is likely that some of the differences we observe between the BV2 cell lysate and retinal lysate are due to other cell types in the retina contributing to the larger effect observed *in vivo*, in addition, recent transcriptome sequencing studies have shown many differences between BV2 cells and primary microglia (Das et al., 2016; He et al., 2018) and as such future studies examining these markers in primary microglia vs BV2 cells would be beneficial. However, despite the limitations of the BV2 microglia cell line the BV2 transcriptomic analysis supports the analysis from the mouse retinal samples in terms of the main DAM markers LPL and APOE, indicating that minocycline is having a targeted effect on lipid metabolism in microglia.

Remarkably, many genes associated with both the first (*Tyrobp*, *Apoe* and *Ctsb*) and second stage (*Lpl, Csf1r and Clec7a*) of DAM activation were down-regulated with minocycline treatment in the retinas from *Rho*$^{-/-}$ animals and/or BV2 microglia. TYROBP is a cytoplasmic adaptor protein for the immunoreceptor TREM2, and this signalling complex promotes Aβ clearance, enhancing microglial phagocytosis while supressing inflammatory cytokine production and secretion from these cells (Ma et al., 2015). Furthermore, triggering of this receptor induces APOE activation, and the APOE-TREM2 signalling pathway has been shown to be a critical regulator of microglia phenotypic change in neurodegenerative disease (Krasemann et al., 2017). Intriguingly, a recent study has reported possible APOE-TYROBP signalling independent of TREM2 and propose that this pathway could be an early or initiating step in DAM activation (Audrain et al., 2021). Although, *Trem2* levels remained unchanged, both *Apoe* and *Tyrobp* levels decreased with minocycline treatment, suggesting that minocycline could reduce TYROBP levels, leading to decreased TREM2 activation and in turn reduced APOE-TREM2 signalling, halting DAM phenotype

activation. Additionally, minocycline could also reduce this recently reported APOE-TYROBP signalling directly, dampening the initiation of DAM.

Upregulation of phagocytic and lipid metabolism genes are characteristic of stage two DAM activation suggesting a preference of lipids to fuel the greater bioenergetics needs of these phagocytic microglia (Loving and Bruce, 2020). Indeed, knockdown of LPL in BV2 cells has previously been shown to reduce microglial phagocytosis of Aβ (Ma et al., 2013). Here, we found that minocycline reduced LPL levels in *Rho*$^{-/-}$ retina and in BV2 microglia both at the transcriptional and protein level. *Clec7a*, the gene encoding the pattern recognition receptor, Dectin-1, is a known inducer of LC3-associated phagocytosis (Ma et al., 2012) and although expressed at very low levels in the *Rho*$^{-/-}$ retina and BV2 microglia, minocycline also significantly reduced *Clec7a* expression.

Lgals3, the gene encoding Galectin-3, and *Itgax* (Integrin subunit alpha X), encoding CD11c were two DAM genes surprisingly increased with minocycline in the *Rho*$^{-/-}$ retinas. Galectin-3 has been found to be highly upregulated in the brains of neurodegenerative disease and was recently identified as a novel endogenous TREM2 ligand (Boza-Serrano, Ruiz et al., 2019). Although an increase in *Lgals3* was observed transcriptionally in *Rho*$^{-/-}$ retinas, this galectin is also expressed in other retinal cells such as Muller glia, and indeed, minocycline failed to alter both *Lgals3* transcriptional and Galectin-3 protein levels in the BV2 microglia cells. Similarly, *Itgax* which is also expressed in vascular endothelial cells and Muller glia, remained unchanged in minocycline-treated BV2 cells.

As many of the DAM genes minocycline targeted were involved in phagocytosis, we examined the basal phagocytic capacity of microglia *in vitro* and found that minocycline reduced microglial phagocytosis in these cells. Indeed, this is also supported by a recent study showing minocycline's ability to reduce the phagocytosis of lipofuscin in primary microglia (Leclaire et al., 2019). Furthermore, we discovered that these minocycline-treated microglia, which had a reduced phagocytic capacity and DAM phenotype, could attenuate photoreceptor cell loss in the *Rho*$^{-/-}$ model of retinal degeneration. *Rho*$^{-/-}$ mice that were administered with minocycline from P16-42, had delayed retinal thinning than vehicle injected mice when examined by analysis of H&E stained retinal sections.

Overall, our data supports other studies demonstrating the therapeutic efficacy of minocycline in retinal degeneration; minocycline treatment has previously been shown to preserve the morphology and function of photoreceptors in the *Rd10* mouse model (Peng et al., 2014), in a light-damage-induced RD model (Scholz et al., 2015) and more recently, in the *Mertk*$^{-/-}$ mouse model of RD (Terauchi et al., 2021). It is important to consider, however, that triggering early DAM activation may be useful to induce a microglia response in diseases where a strong phagocytic activity might be beneficial. Indeed, a recent study using single-cell RNA sequencing to characterize the transcriptome of sub-retinal microglia (srMG) in a light damage model of photoreceptor degeneration as well as a genetic model (*Rho*$^{P23H/WT}$) of chronic retinal degeneration (O'Koren et al., 2019) found that the srMG expressing many DAM markers protected the RPE from disease-associated damage in both models. Additionally, in a model of acute retinal detachment, microglia have been shown to be protective, by rapidly phagocytosing damaging cell debris to avoid triggering apoptosis of neighbouring photoreceptors and also by its close association and control of macrophage infiltration (Okunuki et al., 2018). However, their appearance in our *Rho*$^{-/-}$ model indicate that these mechanisms may be disadvantageous under different conditions. The appearance of LPL on reaching the SRS may give microglia an enhanced phagocytic capacity which may cause premature phagocytosis of otherwise functional photoreceptor cells/segments. Phagocytosis of damaged and dying photoreceptors is important to protect neighbouring healthy cells but overt phagocytosis may enable retinal degeneration to advance at a more progressive rate than otherwise possible.

As microglia participate in vital physiological functions in the retina, complete obliteration or blocking of all retinal microglial functions is undesirable (Wang et al., 2016). Therefore, immunotherapeutic approaches that focus on targeting specific aspects of the microglial phagocytic pathway, e.g. LPL, TYROBP, may be of benefit. Alternatively, targeting the lipid catabolism pathway directly may provide another therapeutic avenue. Furthermore, dampening these over-reactive microglia with minocycline in combination with drugs that target photoreceptor cell death, or promote cell survival pathways, may present a broadly applicable therapy more readily accessible for people with inherited retinopathies.

5. Conclusions

Overall, our study provides compelling evidence that targeting excessive microglia phagocytosis may be a druggable intervention for some retinal degenerative diseases, and we identify many DAM markers, in particular those associated with lipid metabolism, that are down-regulated by minocycline, suggesting that suppression of this pathway may be a mechanism by which minocycline protects against inflammation-induced photoreceptor cell death.

Ethical approval

All animal studies carried out in the Smurfit Institute of Genetics in TCD adhere to the principles laid out by the internal ethics committee at TCD, and all relevant national licenses were obtained before commencement of all studies.

Consent for publication

Not applicable.

Availability of data and materials

Data sharing not applicable to this article aS no datasets were generated during this current study.

Funding

SFI-15 CDA/3497, SFI-18/TIDA/6067, IRCLA/2017/295, HRB/MRCG-2018-08, NCRC/18/10, ERC (Retina Rhythm – 864522).

Authors contributions

EO and CD performed experiments and analysed data, SD directed the research. EO, MC and SD wrote the manuscript. All authors read and approved the final manuscript.

Declaration of competing interest

The authors declare that they have no competing interests.

Acknowledgements

Not applicable.

Appendix A. Supplementary data

Supplementary data to this article can be found online at https://doi.org/10.1016/j.exer.2022.108953.

References

Audrain, M., Haure-Mirande, J.V., Mleczko, J., Wang, M., Griffin, J.K., St George-Hyslop, P.H., Fraser, P., Zhang, B., Gandy, S., Ehrlich, M.E., 2021. Reactive or

transgenic increase in microglial TYROBP reveals a TREM2-independent TYROBP-APOE link in wild-type and Alzheimer's-related mice. Alzheimers Dement 17 (2), 149–163.

Buttgereit, A., Lelios, I., Yu, X., Vrohlings, M., Krakoski, N.R., Gautier, E.L., Nishinakamura, R., Becher, B., Greter, M., 2016. Sall1 is a transcriptional regulator defining microglia identity and function. Nat. Immunol. https://doi.org/10.1038/ni.3585.

Dannhausen, K., Möhle, C., Langmann, T., 2018. Immunomodulation with minocycline rescues retinal degeneration in juvenile neuronal ceroid lipofuscinosis mice highly susceptible to light damage. Dis. Model Mech. 11 (9).

Das, A., Kim, S.H., Arifuzzaman, S., Yoon, T., Chai, J.C., Lee, Y.S., Park, K.S., Jung, K.H., Chai, Y.G., 2016. Transcriptome sequencing reveals that LPS-triggered transcriptional responses in established microglia BV2 cell lines are poorly representative of primary microglia. J. Neuroinflammation 13 (1), 182.

Di Pierdomenico, J., Scholz, R., Valiente-Soriano, F.J., Sanchez-Migallon, M.C., Vidal-Sanz, M., Langmann, T., Agudo-Barriuso, M., Garcia-Ayuso, D., Villegas-Perez, M.P., 2018. Neuroprotective effects of FGF2 and minocycline in two animal models of inherited retinal degeneration. Invest. Ophthalmol. Vis. Sci. 59 (11), 4392–4403.

Gao, W., Du, J., Chi, Y., Zhu, R., Gao, X., Yang, L., 2021. Minocycline prevents the inflammatory response after retinal detachment, where microglia phenotypes being regulated through A20. Exp. Eye Res. 203, 108403.

He, Y., Yao, X., Taylor, N., Bai, Y., Lovenberg, T., Bhattacharya, A., 2018. RNA sequencing analysis reveals quiescent microglia isolation methods from postnatal mouse brains and limitations of BV2 cells. J. Neuroinflammation 15 (1), 153.

Humphries, M.M., Rancourt, D., Farrar, G.J., Kenna, P., Hazel, M., Bush, R.A., Sieving, P. A., Sheils, D.M., McNally, N., Creighton, P., Erven, A., Boros, A., Gulya, K., Capecchi, M.R., Humphries, P., 1997. Retinopathy induced in mice by targeted disruption of the rhodopsin gene. Nat. Genet. 15 (2), 216–219.

Karperien, A., Ahammer, H., Jelinek, H.F., 2013. Quantitating the subtleties of microglial morphology with fractal analysis. Front. Cell. Neurosci. 7, 3.

Keren-Shaul, H., Spinrad, A., Weiner, A., Matcovitch-Natan, O., Dvir-Szternfeld, R., Ulland, T.K., David, E., Baruch, K., Lara-Astaiso, D., Toth, B., Itzkovitz, S., Colonna, M., Schwartz, M., Amit, I., 2017. A unique microglia type Associated with restricting development of Alzheimer's disease. Cell 169 (7), 1276–1290 e1217.

Kobayashi, K., Imagama, S., Ohgomori, T., Hirano, K., Uchimura, K., Sakamoto, K., Hirakawa, A., Takeuchi, H., Suzumura, A., Ishiguro, N., Kadomatsu, K., 2013. Minocycline selectively inhibits M1 polarization of microglia. Cell Death Dis. 4 (3), e525.

Kohno, H., Chen, Y., Kevany, B.M., Pearlman, E., Miyagi, M., Maeda, T., Palczewski, K., Maeda, A., 2013. Photoreceptor proteins initiate microglial activation via Toll-like receptor 4 in retinal degeneration mediated by all-trans-retinal. J. Biol. Chem. 288 (21), 15326–15341.

Krasemann, S., Madore, C., Cialic, R., Baufeld, C., Calcagno, N., El Fatimy, R., Beckers, L., O'Loughlin, E., Xu, Y., Fanek, Z., Greco, D.J., Smith, S.T., Tweet, G., Humulock, Z., Zrzavy, T., Conde-Sanroman, P., Gacias, M., Weng, Z., Chen, H., Tjon, E., Mazaheri, F., Hartmann, K., Madi, A., Ulrich, J.D., Glatzel, M., Worthmann, A., Heeren, J., Budnik, B., Lemere, C., Ikezu, T., Heppner, F.L., Litvak, V., Holtzman, D. M., Lassmann, H., Weiner, H.L., Ochando, J., Haass, C., Butovsky, O., 2017. The TREM2-APOE pathway drives the transcriptional phenotype of dysfunctional microglia in neurodegenerative diseases. Immunity 47 (3), 566–581 e569.

Leclaire, M.D., Nettels-Hackert, G., Konig, J., Hohn, A., Grune, T., Uhlig, C.E., Hansen, U., Eter, N., Heiduschka, P., 2019. Lipofuscin-dependent stimulation of microglial cells. Graefes Arch. Clin. Exp. Ophthalmol. 257 (5), 931–952.

Lew, D.S., Mazzoni, F., Finnemann, S.C., 2020. Microglia inhibition delays retinal degeneration due to MerTK phagocytosis receptor deficiency. Front. Immunol. 11, 1463.

Loving, B.A., Bruce, K.D., 2020. Lipid and lipoprotein metabolism in microglia. Front. Physiol. 11, 393.

Ma, J., Becker, C., Lowell, C.A., Underhill, D.M., 2012. Dectin-1-triggered recruitment of light chain 3 protein to phagosomes facilitates major histocompatibility complex class II presentation of fungal-derived antigens. J. Biol. Chem. 287 (41), 34149–34156.

Ma, J., Jiang, T., Tan, L., Yu, J.T., 2015. TYROBP in Alzheimer's disease. Mol. Neurobiol. 51 (2), 820–826.

Ma, Y., Bao, J., Zhao, X., Shen, H., Lv, J., Ma, S., Zhang, X., Li, Z., Wang, S., Wang, Q., Ji, J., 2013. Activated cyclin-dependent kinase 5 promotes microglial phagocytosis of fibrillar β-amyloid by up-regulating lipoprotein lipase expression. Mol. Cell. Proteomics 12 (10), 2833–2844.

Murakami, Y., Ishikawa, K., Nakao, S., Sonoda, K.H., 2020. Innate immune response in retinal homeostasis and inflammatory disorders. Prog. Retin. Eye Res. 74, 100778.

O'Koren, E.G., Yu, C., Klingeborn, M., Wong, A.Y.W., Prigge, C.L., Mathew, R., Kalnitsky, J., Msallam, R.A., Silvin, A., Kay, J.N., Bowes Rickman, C., Arshavsky, V. Y., Ginhoux, F., Merad, M., Saban, D.R., 2019. Microglial function is distinct in different anatomical locations during retinal homeostasis and degeneration. Immunity 50 (3), 723–737 e727.

Okunuki, Y., Mukai, R., Pearsall, E.A., Klokman, G., Husain, D., Park, D.H., Korobkina, E., Weiner, H.L., Butovsky, O., Ksander, B.R., Miller, J.W., Connor, K.M., 2018. Microglia inhibit photoreceptor cell death and regulate immune cell infiltration in response to retinal detachment. Proc. Natl. Acad. Sci. U. S. A. 115 (27), E6264–E6273.

Ozaki, E., Gibbons, L., Neto, N.G., Kenna, P., Carty, M., Humphries, M., Humphries, P., Campbell, M., Monaghan, M., Bowie, A., Doyle, S.L., 2020. SARM1 deficiency promotes rod and cone photoreceptor cell survival in a model of retinal degeneration. Life Sci. Alliance 3 (5).

Peng, B., Xiao, J., Wang, K., So, K.F., Tipoe, G.L., Lin, B., 2014. Suppression of microglial activation is neuroprotective in a mouse model of human retinitis pigmentosa. J. Neurosci. 34 (24), 8139–8150.

Scholz, R., Sobotka, M., Caramoy, A., Stempfl, T., Moehle, C., Langmann, T., 2015. Minocycline counter-regulates pro-inflammatory microglia responses in the retina and protects from degeneration. J. Neuroinflammation 12, 209.

Silverman, S.M., Ma, W., Wang, X., Zhao, L., Wong, W.T., 2019. C3- and CR3-dependent microglial clearance protects photoreceptors in retinitis pigmentosa. J. Exp. Med. 216 (8), 1925–1943.

Terauchi, R., Kohno, H., Watanabe, S., Saito, S., Watanabe, A., Nakano, T., 2021. Minocycline decreases CCR2-positive monocytes in the retina and ameliorates photoreceptor degeneration in a mouse model of retinitis pigmentosa. PLoS One 16 (4), e0239108.

Wang, X., Zhao, L., Zhang, J., Fariss, R.N., Ma, W., Kretschmer, F., Wang, M., Qian, H.H., Badea, T.C., Diamond, J.S., Gan, W.B., Roger, J.E., Wong, W.T., 2016. Requirement for microglia for the maintenance of synaptic function and integrity in the mature retina. J. Neurosci. 36 (9), 2827–2842.

Zabel, M.K., Zhao, L., Zhang, Y., Gonzalez, S.R., Ma, W., Wang, X., Fariss, R.N., Wong, W. T., 2016. Microglial phagocytosis and activation underlying photoreceptor degeneration is regulated by CX3CL1-CX3CR1 signaling in a mouse model of retinitis pigmentosa. Glia 64 (9), 1479–1491.

Zhang, C., Lei, B., Lam, T.T., Yang, F., Sinha, D., Tso, M.O., 2004. Neuroprotection of photoreceptors by minocycline in light-induced retinal degeneration. Invest. Ophthalmol. Vis. Sci. 45 (8), 2753–2759.

Zhao, L., Zabel, M.K., Wang, X., Ma, W., Shah, P., Fariss, R.N., Qian, H., Parkhurst, C.N., Gan, W.B., Wong, W.T., 2015. Microglial phagocytosis of living photoreceptors contributes to inherited retinal degeneration. EMBO Mol. Med. 7 (9), 1179–1197.